Transl. Stroke Res. (2014) 5:238–247
DOI 10.1007/s12975-014-0333-2

ORIGINAL ARTICLE

Tenascin-C Causes Neuronal Apoptosis After Subarachnoid Hemorrhage in Rats

Masato Shiba · Masashi Fujimoto · Kyoko Imanaka-Yoshida · Toshimichi Yoshida · Waro Taki · Hidenori Suzuki

Received: 2 November 2013 / Revised: 15 January 2014 / Accepted: 16 January 2014 / Published online: 1 February 2014

Abstract The role of tenascin-C (TNC), a matricellular protein, in brain injury is unknown. The aim of this study was to examine if TNC causes neuronal apoptosis after subarachnoid hemorrhage (SAH), a deadly cerebrovascular disorder, using imatinib mesylate (a selective inhibitor of platelet-derived growth factor receptor [PDGFR] that is reported to suppress TNC induction) and recombinant TNC. SAH by endovascular perforation caused caspase-dependent neuronal apoptosis in the cerebral cortex irrespective of cerebral vasospasm development at 24 and 72 h post-SAH, associated with PDGFR activation, mitogen-activated protein kinases (MAPKs) activation, and TNC induction in rats. PDGFR inactivation by an intraperitoneal injection of imatinib mesylate prevented neuronal apoptosis, as well as MAPKs activation and TNC induction in the cerebral cortex at 24 h. A cisternal injection of recombinant TNC reactivated MAPKs and abolished anti-apoptotic effects of imatinib mesylate. The TNC injection also induced TNC itself in SAH brain, which may internally augment neuronal apoptosis after SAH. These findings suggest that TNC upregulation by PDGFR activation causes neuronal apoptosis via MAPK activation, and that the positive feedback mechanisms may exist to augment neuronal apoptosis after SAH. TNC-induced neuronal apoptosis would be a new target to improve outcome after SAH.

Keywords Tenascin-C · Neuronal apoptosis · Early brain injury · Subarachnoid hemorrhage

Introduction

Tenascin-C (TNC) is one of matricellular proteins, which are the family of non-structural and secreted extracellular matrix proteins [1]. The expression of TNC is extremely limited in normal adult tissues, but is induced rapidly and profusely by inflammatory or noxious stimuli [2]. TNC exerts various functions including the regulation of cell migration, proliferation, and apoptosis, reported to be involved in tissue remodeling [3]. Recently, some clinical studies reported that TNC was induced in serum and cerebrospinal fluid after subarachnoid hemorrhage (SAH), a deadly cerebrovascular disorder, associated with cerebral vasospasm and poor outcomes [4, 5]. A recent experimental study reported that post-SAH TNC expression in the arterial wall caused cerebral vasospasm in rats [6]. However, the significance of TNC induction after SAH remains unclear, especially in brain tissue.

Existing evidence suggests that many factors including early brain injury as well as cerebral vasospasm cause poor outcome after SAH [7], and that early brain injury may be more important and earlier manifestation of brain injuries causing delayed neurological deterioration after SAH [8]. Recent studies showed that neuronal apoptosis is an important component of early brain injury [9]. As TNC was reported to be proapoptotic for cultured smooth muscle cells [10], we hypothesized that TNC causes post-SAH neuronal apoptosis. However, no study has investigated the role of TNC in neuronal apoptosis or brain injury in any animal model. Thus, in this study, we used a SAH model by endovascular perforation,

Electronic supplementary material The online version of this article (doi:10.1007/s12975-014-0333-2) contains supplementary material, which is available to authorized users.

M. Shiba · M. Fujimoto · W. Taki · H. Suzuki (✉)
Department of Neurosurgery, Mie University Graduate School of Medicine, 2-174 Edobashi, Tsu, Mie 514-8507, Japan
e-mail: mie1192suzuki@gmail.com

K. Imanaka-Yoshida · T. Yoshida
Department of Pathology and Matrix Biology, Mie University Graduate School of Medicine, Tsu, Japan

K. Imanaka-Yoshida · T. Yoshida · H. Suzuki
Research Center for Matrix Biology, Mie University Graduate School of Medicine, Tsu, Japan

which shows a high mortality and acute metabolic changes similar to clinical findings [11], and for the first time examined if TNC causes neuronal apoptosis using imatinib mesylate (imatinib, a selective inhibitor of the tyrosine kinases of platelet-derived growth factor [PDGF] receptors [PDGFRs]) and recombinant TNC treatments, because there are neither inhibitors nor neutralizing antibodies specific for TNC but imatinib suppressed TNC induction at least for 24 h post-SAH [6].

Materials and Methods

All procedures were approved by the Animal Ethics Review Committee of Mie University, and were in accordance with the institution's Guidelines for Animal Experiments.

SAH Model and Study Protocol

The endovascular perforation model of SAH was produced in male adult Sprague-Dawley rats (age 8–9 weeks, 270–320 g; SLC, Hamamatsu, Japan) as previously described [6]. Each animal was anesthetized by an intraperitoneal injection of 4 % chloral hydrate (10 ml/kg). A sharpened 4–0 monofilament nylon suture was advanced rostrally into the left internal carotid artery from the external carotid artery stump to perforate the bifurcation of the left anterior and middle cerebral arteries (MCAs). Blood pressure and blood gas were measured via the left femoral artery. Rectal temperature was kept at 37 °C during surgery. Sham-operated rats underwent identical procedures except that the suture was withdrawn without puncture.

First, 98 rats underwent endovascular perforation SAH or sham operation. After 30 min, the 58 surviving rats were randomly divided into three groups (Fig. 1a), and 50 mg/kg body weight of imatinib (Novartis, Basel, Switzerland) or vehicle (phosphate-buffered saline [PBS], 10 mL/kg) was administered intraperitoneally. The dosage of imatinib in this study was determined based on our previous study that tested effects of two dosages (10 and 50 mg/kg) of imatinib on cerebral vasospasm [6]. Neuronal apoptosis and vasospasm were evaluated at 24–72 h post-surgery.

Next, 2 μg of recombinant TNC or vehicle (PBS, 100 μL) was injected into the cisterna magna in rats. After 30 min, SAH was produced and SAH rats were treated with 50 mg/kg of imatinib as above. Randomization into either TNC or vehicle-treated SAH-imatinib groups was continued until the number of animals per group reached ≥6. All evaluations were performed at 24 h post-SAH (Fig. 1b).

Neurobehavioral Test

Neurological impairments were blindly evaluated using the neurological scores. Neurological scores (3–18 points) were assessed by summing up six test scores (spontaneous activity;

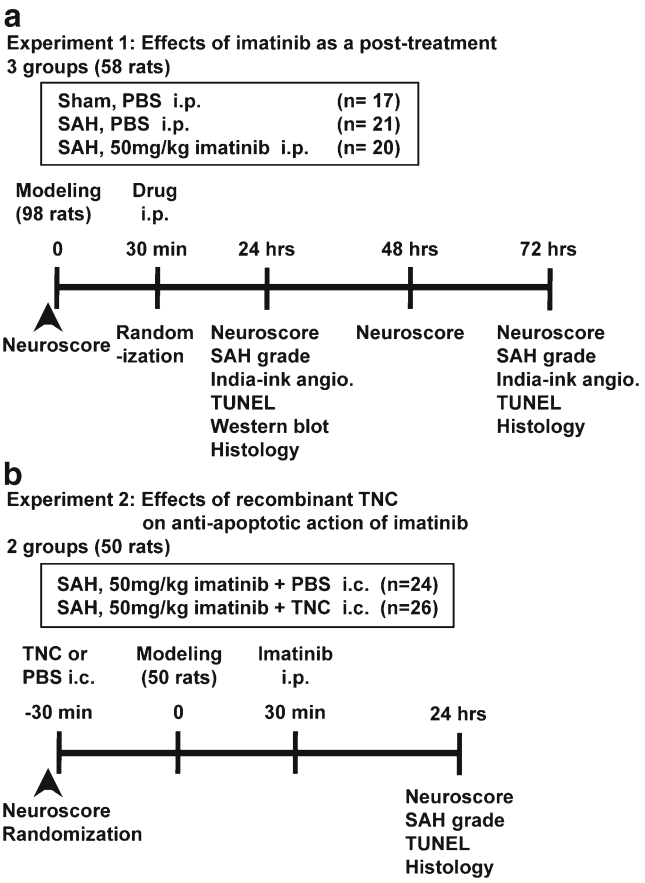

Fig. 1 Experimental designs. Experiment 1 (**a**) was designed to examine effects of post-SAH treatment of imatinib on vasospasm and neuronal apoptosis; experiment 2 (**b**) to examine if recombinant TNC causes neuronal apoptosis in imatinib-treated SAH rats. *Angio*. angiography, *i.c.* intracisternal injection, *i.p.* intraperitoneal injection, *PBS* phosphate-buffered saline, *TUNEL* terminal deoxynucleotidyltransferase-mediated dUTP nick-end labeling staining

spontaneous movement of four limbs; forepaw outstretching; climbing; body proprioception; and response to whisker stimulation) as previously described [12]. Higher scores indicate greater function.

Severity of SAH

The severity of SAH was blindly assessed at each sacrifice as previously described [12]. The basal cistern was divided into six segments, and each segment was allotted a grade from 0 to 3 depending on the amount of SAH. The animals received a total score ranging from 0 to 18 by summing up the scores.

Intracisternal Infusion

Using a surgical microscope (Zeiss, Germany), the posterior cervical muscles were dissected through a suboccipital midline skin incision, and the atlanto-occipital membrane was exposed [13]. The membrane was penetrated by a 27-gauge needle. Sterile PBS vehicle (100 μL) or mouse recombinant

TNC (murine myeloma cell line, NS0-derived, Gly23–Pro625, with a C-terminal 6-His tag, 2 μg in 100 μL; R&D Systems, Minneapolis, MN) was infused at a rate of 100 μL/min irrespective of the animal's body weight at 30 min pre-surgery as previously described [6]. The needle was removed 10 min after an infusion, and the pore was quickly plugged with oxidized cellulose.

India Ink Angiography

Gelatin-India ink solution was made by dissolving gelatin powder (7 g) in 100 mL PBS and mixing with 100 mL India ink (Kuretake Co, Nara, Japan) [14]. The ascending aorta was cannulated with a blunted 16-gauge needle attached to flexible plastic tubing, which was connected to a pressure transducer (Nihon Kohden Co, Tokyo, Japan) and a syringe on an automatic infusion pump. After an incision was made in the right atrium to allow for the outflow of perfusion solutions, 100 mL of PBS, 15 min of 10 % formalin, and 10 min of 3.5 % gelatin-India ink solution were infused through the closed circuit. All perfusates were passed through a 0.2-μm pore size filter and delivered at 60–80 mmHg. The rat was refrigerated at 4 °C for 24 h to allow gelatin solidification. The brains were harvested and high-resolution pictures of the circle of Willis were taken with a scale before and after the removal of a subarachnoid clot. The brain was stored in 10 % neutral buffered formalin for terminal deoxynucleotidyltransferase-mediated dUTP nick-end labeling (TUNEL) staining and immunohistochemistry.

An experienced person who was unaware of the treatment groups measured the smallest lumen diameter of sphenoidal segment of the left MCA three times and determined a mean value of the segment.

Western Blot Analyses

Western blot analyses were performed as previously described [15]. The left whole cerebral cortex was harvested under a microscope and homogenized. Equal amounts of protein samples (1 μg) were loaded on SDS-PAGE gels, electrophoresed, and transferred onto a polyvinylidene difluoride membrane. The membranes were blocked with 2 % bovine serum albumin, followed by incubation overnight at 4 °C with the rabbit polyclonal anti-phosphorylated extracellular signal-regulated kinase (ERK) 1/2, mouse monoclonal anti-phosphorylated c-Jun N-terminal kinase (JNK), mouse monoclonal anti-phosphorylated p38 (1:1,000, Santa Cruz Biotechnology, Santa Cruz, CA), rabbit monoclonal anti-PDGFR-α, rabbit monoclonal anti-PDGFR-β (1:1,000, Cell Signaling Technology, Danvers, MA), rabbit polyclonal anti-phosphorylated PDGFR (α: Y572/574, β: Y579/581; 1:1,000, Biosource, Camarillo, CA), mouse monoclonal anti-TNC (0.72 μg/mL, Immuno-Biological Laboratories, Takasaki, Japan) and rabbit polyclonal anti-cleaved caspase-3 (1:1,000, Cell Signaling Technology, Danvers, MA) antibodies. The anti-TNC antibody detected different TNC isoforms: the large (TNC_L, 280 kDa), intermediate-sized (TNC_I, 200 kDa) and small (TNC_S, 190 kDa) variants [16]. Blot bands were detected with a chemiluminescence reagent kit (ECL Prime; Amersham Bioscience, Arlington Heights, IL) and quantified by densitometry with the Image J software in a blind fashion. β-tubulin (1:2,000, Santa Cruz Biotechnology, Santa Cruz, CA) was used as an internal control for every experiment. Changes in the protein expression were expressed as a percentage of the values in sham-operated rats treated with PBS at 24 h/values of β-tubulin.

TUNEL Staining

TUNEL staining was performed as previously described [9]. Four-micrometer-thick coronal sections at the level of bregma+1.0 mm were cut using a microtome and were subjected to TUNEL staining with an in situ cell death detection kit (Roche Inc, Mannheim, Germany). Color reactions were developed in diaminobenzidine/hydrogen peroxide solution and the sections were counterstained with hematoxylin solution for light microscopic examination. Incubation with labeling solution without the enzyme served as a negative labeling control. Intact neurons were morphologically defined by oval nuclei and prominent nucleoli, and degenerating morphology suggesting apoptosis included pyknotic, amorphous, fragmented, or shrunken nuclei [17, 18]. The TUNEL-positive neurons were measured in the left secondary somatosensory cortex (they were counted in 10 non-overlapping fields along the brain surface per case at ×400 magnification and expressed as the mean number of TUNEL-positive neurons per square millimeter) in a blind manner.

Immunohistochemistry

Immunohistochemistry on formalin-fixed paraffin-embedded sections was performed to examine which cells or tissues were immunoreactive for the protein that was shown to increase by Western blotting as described previously [19]. After dewaxing and rehydration, the sections were treated with 3 % hydrogen peroxide for 10 min to block endogenous peroxidase activities, placed in 1 mmol ethylenediaminetetraacetic acid (pH 8.0) and heated in an autoclave at 121 °C for 1 min. The sections were then blocked with 5 % goat or horse serum and incubated overnight at 4 °C with the rabbit polyclonal anti-phosphorylated ERK1/2, mouse monoclonal anti-phosphorylated JNK, mouse monoclonal anti-phosphorylated p38 (1:200, Santa Cruz Biotechnology, Santa Cruz, CA), rabbit polyclonal anti-phosphorylated PDGFR (α: Y572/574, β: Y579/581; 1:200, Biosource, Camarillo, CA),

mouse monoclonal anti-TNC (1 μg/mL, Immuno-Biological Laboratories, Takasaki, Japan), and rabbit polyclonal anti-cleaved caspase-3 (1:200, Cell Signaling Technology, Danvers, MA) antibodies. They were subsequently incubated with biotinylated anti-rabbit or anti-mouse immunoglobulin (Vector Laboratories, Burlingame, CA) for 30 min and then with an avidin-biotin complex for 30 min at room temperature. Color reactions were developed in diaminobenzidine/hydrogen peroxide solution and the sections were counterstained with hematoxylin solution for light microscopic examination. Negative controls consisted of serial sections incubated with buffer alone instead of the primary antibodies.

Statistics

Neurological scores were expressed as median±25th–75th percentiles, and were analyzed using Mann–Whitney *U* tests or Kruskal-Wallis tests, followed by Steel-Dwass multiple comparisons. Other values were expressed as mean±standard error of the mean (SEM), and unpaired *t*, chi-square tests and one-way analysis of variance (ANOVA) with Tukey-Kramer post hoc tests were used as appropriate. $P<0.05$ was considered significant.

In the statistical analysis, we calculated the power of the tests. The number of animals per group necessary to reach the desired power of 0.800 was in the range of four to six.

Results

Post-SAH-Imatinib Prevents Neurological Impairments at 24 h, but Not at 48 and 72 h

There were no significant differences in physiological parameters among the groups (data not shown). None of the sham-operated rats died within the 72-h observation period. Forty (49.4 %) of 81 SAH rats died within 30 min after surgery and before the drug injection. The mortality of SAH rats after randomization into either treatment group was not significantly different between the PBS (19.0 %, 4 of 21 rats) and imatinib (15.0 %, 3 of 20 rats) treatment groups (chi-square tests). The average SAH grading score was similar between the PBS and imatinib treatment groups in each analysis at both 24 (14.9±0.5 versus 14.1±0.6, respectively) and 72 (9±1.3 versus 10.8±1.9, respectively)h post-SAH (unpaired *t* tests).

Neurological scores were significantly impaired at 24–72 h after SAH in comparison with the sham groups (Fig. 2). Post-SAH administration of imatinib significantly improved neurological scores at 24 h post-SAH ($P<0.05$) compared with the SAH-vehicle group, but the effect was not observed at 48 and 72 h (Kruskal-Wallis tests; Fig. 2).

Effects of Imatinib on Neuronal Apoptosis and Cerebral Vasospasm

There were many TUNEL-positive neurons seen in the left secondary somatosensory cortex associated with cleaved caspase-3 expressions at 24 and 72 h after SAH (Fig. 3 and Supplementary Fig. 1). The imatinib treatment almost completely prevented the appearance of TUNEL-positive neurons as well as cleaved caspase-3 expressions at 24 h post-SAH. However, the imatinib treatment failed to decrease TUNEL-positive neurons significantly at 72 h (Fig. 3 and Supplementary Fig. 1).

On the other hand, imatinib almost completely prevented vasospasm in the left MCA, which feeds the left secondary somatosensory cortex, at both 24 ($P<0.01$) and 72 ($P<0.05$)h post-SAH compared with the SAH-vehicle groups (ANOVA; Fig. 4).

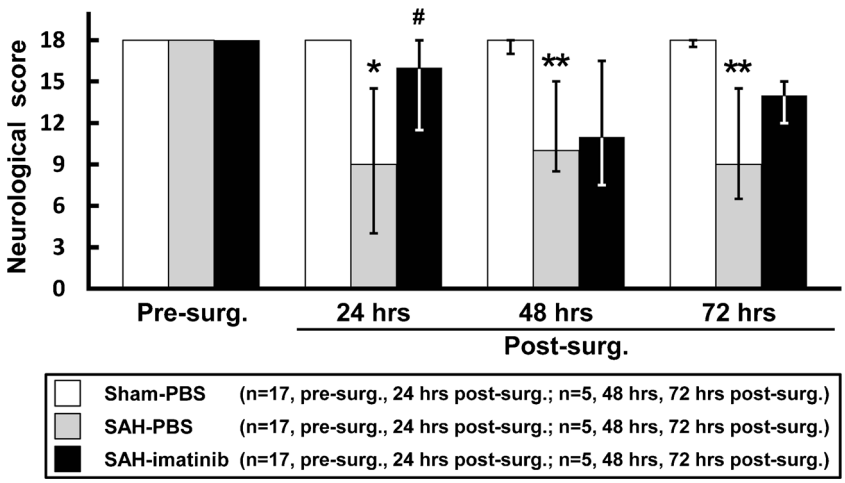

Fig. 2 Effects of post-SAH-imatinib treatment on neurological scores. Data are expressed as median±25th–75th percentiles. *Surg.* surgery, *Sham-PBS* sham-operated rats treated with PBS, *SAH-PBS, SAH-imatinib* SAH rats treated with PBS or imatinib. *$P<0.001$, **$P<0.05$ vs. sham-PBS; #$P<0.05$ vs. SAH-PBS, Kruskal-Wallis tests

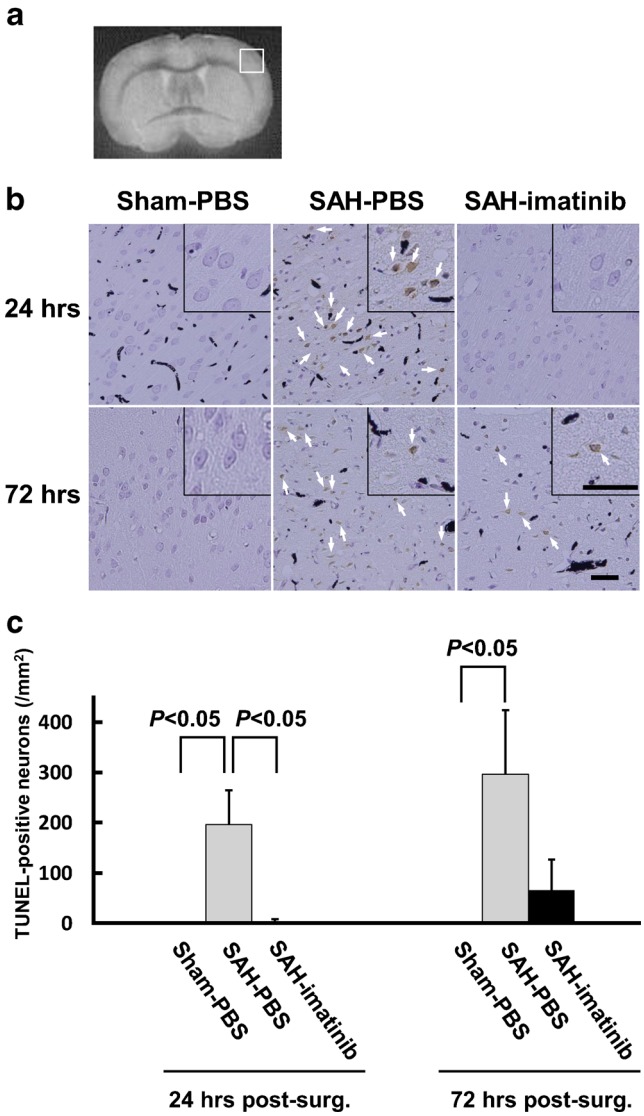

Fig. 3 Effects of post-SAH-imatinib treatment on neuronal apoptosis in the left secondary somatosensory cortex at bregma+1 mm. Representative SAH brain slice showing the left secondary somatosensory cortex (**a**). Representative images showing TUNEL-positive neurons (*arrows*) (**b**) and quantitative analysis of TUNEL-positive neurons (**c**). *Sham-PBS* sham-operated rats treated with PBS, *SAH-PBS, SAH-imatinib* SAH rats treated with PBS or imatinib, *surg.* surgery, *data* mean±SEM; *P* value, ANOVA. *N*=5 per group. *Bar*=50 μm. The *black dots* seen in Fig. 3b indicate India ink in the microvessels, not TUNEL-positive cells (*brown*)

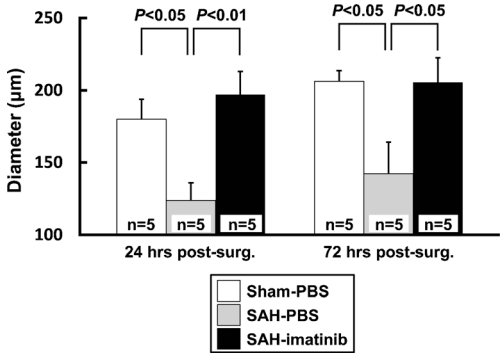

Fig. 4 Effects of post-SAH-imatinib treatment on vessel diameter of the left MCA at 24 and 72 h post-surgery (post-surg.). Data are expressed as mean±SEM. *Sham-PBS* sham-operated rats treated with PBS; *SAH-PBS, SAH-imatinib* SAH rats treated with PBS or imatinib. *P* values, ANOVA

Effects of Imatinib on Protein Expression Changes in Cerebral Cortex

Western blot analyses showed that SAH significantly increased phosphorylated PDGFR, ERK1/2, JNK and p38 levels ($P<0.01$, $P<0.05$, $P<0.001$, and $P<0.01$, respectively) associated with upregulation of TNC_I and TNC_S in the left cerebral cortex at 24 h (Fig. 5 and Supplementary Fig. 2). SAH did not upregulate PDGFRs-α and -β (Fig. 5b). Imatinib significantly dephosphorylated PDGFR and all mitogen-activated protein kinases (MAPKs), and suppressed expression levels of TNC_I and TNC_S at 24 h.

Immunohistochemistry showed that PDGFR in neurons and astrocytes, and ERK1/2 in neurons were activated at both 24 and 72 h post-SAH, while JNK in astrocytes and endothelial cells, and p38 in neurons and endothelial cells were activated only at 24 h post-SAH (Fig. 6). TNC was increased in neuropil mainly in the brain surface of the left secondary somatosensory cortex at both 24 and 72 h. The imatinib treatment remarkably inhibited the immunoreactivities of phosphorylated PDGFR, phosphorylated ERK1/2, phosphorylated JNK, phosphorylated p38 and TNC at 24 h, but the immunoreactivities of phosphorylated PDGFR, phosphorylated ERK1/2 and TNC were not suppressed by the imatinib treatment at 72 h after SAH (Fig. 6).

TNC Injection Reverses Anti-apoptotic Effects of Imatinib

A cisternal injection of recombinant TNC or PBS caused no mortality. However, 13 (54.2 %) of 24 PBS-injected rats and 14 (53.8 %) of 26 TNC-injected rats died after SAH and before imatinib treatment. After the imatinib treatment, the mortality of SAH-imatinib rats was not significantly different between the PBS (45.5 %, 5 of 11 rats) and TNC (50.0 %, 6 of 12 rats) treatment groups (chi-square tests). The average SAH grading score was similar between the PBS (13.5±1.2) and TNC (13.7±0.3) treatment groups (unpaired *t* tests). Intracisternal infusions of recombinant TNC significantly aggravated neurological scores and increased neuronal apoptosis in the left secondary somatosensory cortex compared with the PBS-treated SAH-imatinib group (Fig. 7).

Immunohistochemistry showed that recombinant TNC increased phosphorylated ERK1/2 and p38 in neurons, phosphorylated JNK in astrocytes, phosphorylated JNK and p38 in endothelial cells, and TNC expressions in neuropil in the left secondary somatosensory cortex (Supplementary Fig. 3).

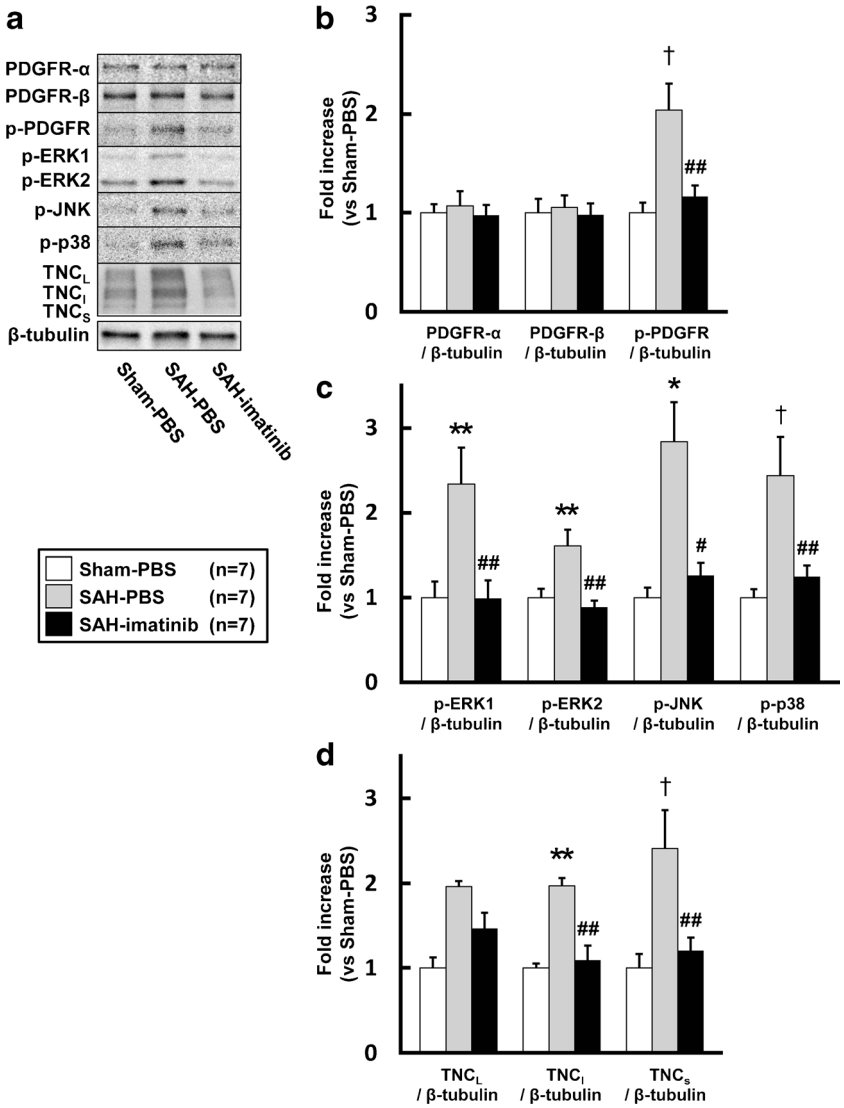

Fig. 5 Representative Western blots (**a**) and effects of post-SAH-imatinib treatment on expression of PDGFRs (**b**), phosphorylated MAPKs (**c**) and TNC (**d**) in the left cerebral cortex at 24 h post-SAH. Expression levels of each protein are expressed as mean± SEM. *Sham-PBS* sham-operated rats treated with PBS, *SAH-PBS, SAH-imatinib* SAH rats treated with PBS or imatinib, *p-PDGFR* phosphorylated PDGFR, *p-ERK1/2* phosphorylated ERK1/2, *p-JNK* phosphorylated JNK, *p-p38* phosphorylated p38. *$P<0.001$, $^{\dagger}P<0.01$, **$P<0.05$ vs. sham-PBS; $^{\#}P<0.01$, $^{\#\#}P<0.05$ vs. SAH-PBS, ANOVA

Discussion

In the present study, we first demonstrated that SAH activated PDGFR and upregulated TNC in the cerebral cortex with MAPK activation and induction of neuronal apoptosis. Imatinib prevented all of neuronal apoptosis, vasospasm and neurobehavioral impairments at 24 h post-SAH; in contrast, imatinib prevented only vasospasm, but neither neuronal apoptosis nor neurobehavioral impairments at 72 h. These findings suggest that neuronal apoptosis is more important than vasospasm as a cause of neurobehavioral impairments in the endovascular perforation model of SAH, because neurobehavioral impairments were associated with neuronal apoptosis, but not with vasospasm. In addition, these findings show that neuronal apoptosis occurred independently of vasospasm development, and that neuronal apoptosis not secondary to vasospasm caused neuronal impairments, supporting recent research efforts that focus on early brain injury to improve outcome after SAH [7]. Imatinib, a PDGFR inhibitor, prevented TNC upregulation, MAPK activation, and neuronal apoptosis. Recombinant TNC injections reactivated MAPKs and abolished anti-apoptotic effects of imatinib, demonstrating that TNC is a mediator of post-SAH neuronal apoptosis through the mechanism of PDGF and MAPKs. Moreover, TNC injections induced TNC itself in SAH brain, suggesting the existence of the positive feedback mechanisms to augment neuronal apoptosis (Fig. 8).

Recent randomized clinical trials showed that clazosentan significantly prevented angiographic vasospasm but failed to improve neurological outcome [20–22]. The studies have made research efforts moved to early brain injury from vasospasm to improve outcome after SAH [7], although the linkage between early brain injury and outcome has not been demonstrated in a clinical setting yet. Neuronal apoptosis has been involved in the pathogenesis of early brain injury after experimental SAH and in a clinical setting [7, 9]. We

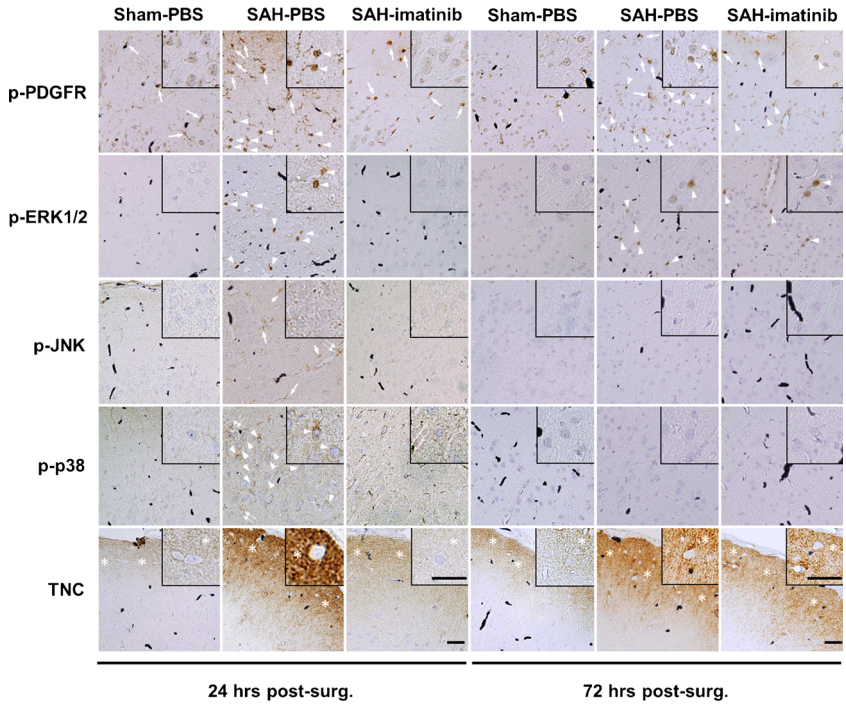

Fig. 6 Effects of post-SAH-imatinib treatment on immunohistochemical stainings of phosphorylated PDGFR (*p-PDGFR*), phosphorylated MAPKs and TNC in the left secondary somatosensory cortex at bregma+1 mm at 24 and 72 h post-surgery (*post-surg.*). *Sham-PBS* sham-operated rats treated with PBS, *SAH-PBS, SAH-imatinib* SAH rats treated with PBS or imatinib, *p-ERK1/2* phosphorylated ERK1/2, *p-JNK* phosphorylated JNK, *p-p38* phosphorylated p38. *Arrows* immunoreactive astrocytes, *arrowheads* immunoreactive neurons, *double arrows* immunoreactive endothelial cells, *asterisks* neuropil. *Upper right panels of each figure* magnification of neurons. *Bar* 50 μm

recently reported that imatinib prevented cerebral vasospasm via inhibiting TNC expression in the arterial wall after SAH [6]. This study demonstrated that imatinib also prevented neuronal apoptosis via inhibiting TNC induction in brain at 24 h, but failed to block TNC induction in brain and therefore neuronal apoptosis, resulting in no significant neurological improvement at 72 h post-SAH, irrespective of almost complete inhibition of vasospasm (imatinib might inhibit TNC induction only in the cerebral artery, but not in the brain at 72 h post-SAH). These findings showed the importance of neuronal apoptosis in post-SAH neurological impairments as well as potential effectiveness of imatinib on both vasospasm and neuronal apoptosis. Because this study tested only immediate one-time treatment with imatinib after SAH, it would be worthwhile examining the effects of multiple treatments at different dosages or time courses on both vasospasm and neuronal apoptosis.

TNC, a matricellular protein, is highly expressed in embryonic tissue during morphogenesis [2, 23] and has multiple functions in the regulation of cell migration, proliferation, and apoptosis [3]. TNC is composed of six subunits, and each subunit includes three types of structural modules: epidermal growth factor-like repeats, fibronectin type III repeats and fibrinogen-like sequence [2, 24]. Alternative splicing of the TNC transcript generates structurally and functionally different isoforms: TNC_L, TNC_I, and TNC_S variants [16]. These variants exhibit differences in deposition site, receptor binding, and biological function [16]. However, functions of these variants in rat brain remain unknown. This study suggested that TNC_I and TNC_S may be more important for post-SAH neuronal apoptosis, but further studies are needed to clarify the role of each TNC variant in SAH brain.

TNC potentially binds to various cell adhesion receptors, for example, epidermal growth factor receptor, integrin, toll-like receptor 4 and so on [25]. Upon binding to these partners, TNC exerts various functions such as activating MAPKs [25]. MAPKs have been reported to induce neuronal apoptosis [26]. Recent studies demonstrated that neuronal apoptosis occurred through the activation of ERK1/2 at 7 days in the cisternal double hemorrhage model of SAH in rats [27], and through the activation of JNK at 24 h in the endovascular perforation model of SAH in rats [19]. Additionally, p38 was reported to be involved in the mechanisms of blood–brain barrier disruption at 24 h in the endovascular perforation model of SAH in rats [28]. This study suggested that post-SAH neuronal apoptosis occurred via the activation of ERK1/2 and p38 at 24 h, and via ERK1/2 activation at 72 h. Recombinant TNC injections also activated ERK1/2 and p38 in neurons, and caused neuronal apoptosis at 24 h post-injection (Fig. 8). On the other hand, MAPKs are well known to have a dual role [26]. Thus, further studies are needed to examine if activation of each isoform of MAPKs in different cells is an epiphenomenon or has beneficial or deleterious effects on outcome in the setting of this study, although the diverse expression and role of MAPKs in post-SAH brain may be explained by limited injury with an irregular pattern in the cerebral cortex.

PDGF is a strong inducer of TNC [29], and PDGFR is expressed and phosphorylated on astrocytes [30] and neurons [31]. Cultured astrocytes secreted TNC in response to serum stimulation, and TNC in turn activated astrocytes itself

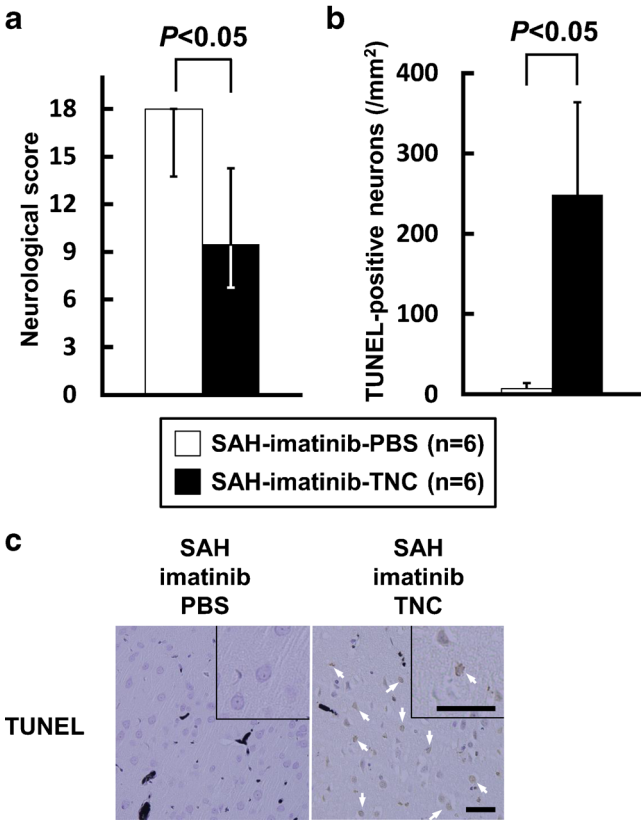

Fig. 7 Effects of intracisternal infusions of recombinant TNC on neurological scores (**a**) and neuronal apoptosis in the left secondary somatosensory cortex (**b** cell counting; **c** representative images) in SAH rats treated with imatinib (SAH-imatinib) at 24 h post-SAH. Data are expressed as median±25th–75th percentiles (**a**) or mean±SEM (**b**). *SAH-imatinib-PBS or -TNC* SAH-imatinib with a pre-SAH intracisternal infusion of PBS or TNC. *P* values: **a** Mann–Whitney *U* tests, **b** unpaired *t* tests. *Arrows* apoptotic neurons. *Upper right panels of each figure* magnification of neurons. *Bar* 50 μm

through a paracrine and autocrine mechanism [32]. TNC also upregulated TNC by the activation of MAPKs [23]. In this study, imatinib, a PDGFR inhibitor, blocked TNC upregulation and MAPK activation, while intracisternal infusion of recombinant TNC reactivated MAPKs and re-induced TNC upregulation irrespective of imatinib treatment. Taken together, SAH may upregulate TNC through PDGFR activation in astrocytes and neurons, and TNC in turn may activate MAPKs, which induce neuronal apoptosis while TNC more at least in neurons, astrocytes, and capillary endothelial cells, implying that there is a positive feedback mechanism of TNC to aggravate neuronal apoptosis (Fig. 8).

This study is somewhat limited. First, we did not measure imatinib concentrations in brain tissue, although imatinib is a small molecule derivative of a 2-phenylaminopyrimidine (molecular weight, 589.7 kDa) [33], and has been shown to cross the blood–brain barrier [34]. Secondly, TNC was given via a cisternal injection to allow for easy permeation of TNC into the brain parenchyma. However, this study provided no evidence showing how deeply TNC permeated into the brain parenchyma. Thirdly, this study demonstrated that imatinib, a selective inhibitor of the tyrosine kinases of PDGFRs, prevented neuronal apoptosis associated with suppressing TNC upregulation at 24 h post-SAH. However, a single pharmacological probe (imatinib), a single dose and two time points as well as insufficient negative controls (for example, lack of PBS injection plus imatinib with or without TNC) cannot exclude the possibility that imatinib prevented neuronal apoptosis by TNC-unrelated mechanisms and that imatinib merely delayed the neuronal apoptosis development, although exogenous TNC abolished imatinib's anti-apoptotic

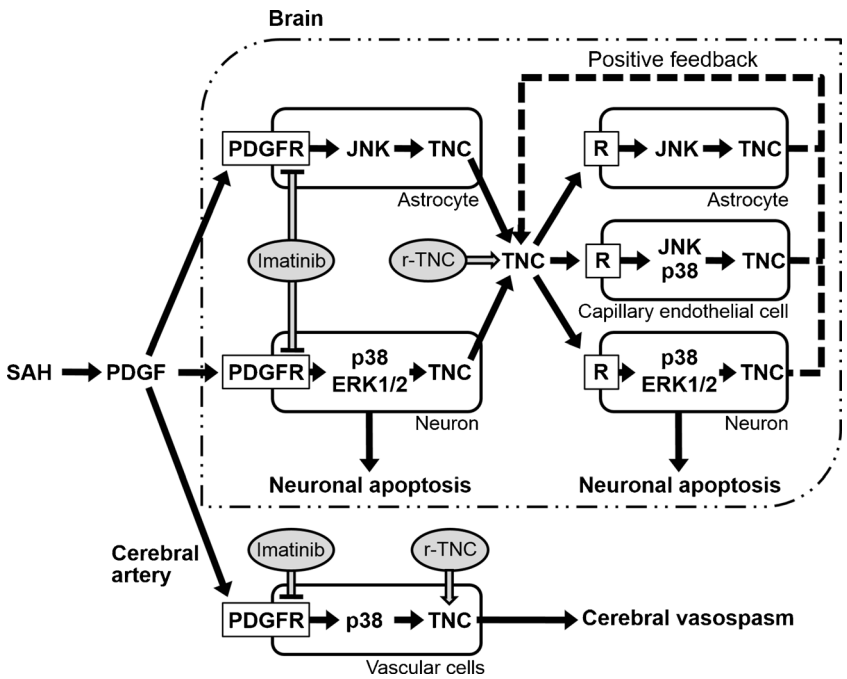

Fig. 8 Possible mechanisms for PDGF, TNC, and MAPK to induce neuronal apoptosis and cerebral vasospasm after SAH. Imatinib blocks PDGFR activation to prevent TNC induction, *R* receptor for TNC, *r-TNC* recombinant TNC

effects. In addition, there are many TNC inducers such as interleukin-1 other than PDGF potentially activated after SAH [2, 15]. To determine if TNC causes post-SAH neuronal apoptosis more exactly, thus, TNC knockout mice may be useful for future studies [35]. Fourthly, neurons and immunoreactive cells were morphologically defined in this study. Although two pathologists qualified the diagnosis, immunohistochemistry should be performed to determine the cell origin of TUNEL-positive cells and the cellular localization of MAPKs more exactly. Lastly, this study showed that one-time treatment with imatinib failed to improve brain injury at 72 h. It would be more useful if multiple treatments at different dosages with imatinib reduced brain injury at later time points, needing time course and dose-finding studies.

In conclusion, we demonstrated for the first time that TNC may play an important role in the pathogenesis of neuronal apoptosis after SAH. Further investigations may prove that TNC provides a novel therapeutic approach against neuronal apoptosis for improving neurological outcome after SAH.

Acknowledgments We thank Ms. Chiduru Yamamoto (Department of Neurosurgery, Mie University Graduate School of Medicine) for her technical assistance.

This work was supported in part by a grant-in-aid for Scientific Research from Japan Society for the Promotion of Science and the NOVARTIS Foundation (Japan) for the Promotion of Science to Dr. Suzuki.

Compliance with Ethics Requirements

Conflict of Interest The authors report no conflicts of interest.

All institutional and national guidelines for the care and use of laboratory animals were followed.

References

1. Matsui Y, Morimoto J, Uede T. Role of matricellular proteins in cardiac tissue remodeling after myocardial infarction. World J Biol Chem. 2010;1:69–80.
2. Chiquet-Ehrismann R, Chiquet M. Tenascins: regulation and putative functions during pathological stress. J Pathol. 2003;200:488–99.
3. Jones PL, Jones FS. Tenascin-C in development and disease: gene regulation and cell function. Matrix Biol. 2000;19:581–96.
4. Suzuki H, Kanamaru K, Shiba M, Fujimoto M, Imanaka-Yoshida K, Yoshida T, et al. Cerebrospinal fluid tenascin-C in cerebral vasospasm after aneurysmal subarachnoid hemorrhage. J Neurosurg Anesthesiol. 2011;23:310–7.
5. Suzuki H, Kanamaru K, Suzuki Y, Aimi Y, Matsubara N, Araki T, et al. Tenascin-C is induced in cerebral vasospasm after subarachnoid hemorrhage in rats and humans: a pilot study. Neurol Res. 2010;32:179–84.
6. Shiba M, Suzuki H, Fujimoto M, Shimojo N, Imanaka-Yoshida K, Yoshida T, et al. Imatinib mesylate prevents cerebral vasospasm after subarachnoid hemorrhage via inhibiting tenascin-C expression in rats. Neurobiol Dis. 2012;46:172–9.
7. Sehba FA, Pluta RM, Zhang JH. Metamorphosis of subarachnoid hemorrhage research: from delayed vasospasm to early brain injury. Mol Neurobiol. 2011;43:27–40.
8. Fujii M, Yan J, Rolland WB, Soejima Y, Caner B, Zhang JH. Early brain injury, an evolving frontier in subarachnoid hemorrhage research. Transl Stroke Res. 2013;4:432–46.
9. Hasegawa Y, Suzuki H, Altay O, Zhang JH. Preservation of tropomyosin-related kinase B (TrkB) signaling by sodium orthovanadate attenuates early brain injury after subarachnoid hemorrhage in rats. Stroke. 2011;42:477–83.
10. Wallner K, Li C, Shah PK, Wu KJ, Schwartz SM, Sharifi BG. EGF-Like domain of tenascin-C is proapoptotic for cultured smooth muscle cells. Arterioscler Thromb Vasc Biol. 2004;24:1416–21.
11. Titova E, Ostrowski RP, Zhang JH, Tang J. Experimental models of subarachnoid hemorrhage for studies of cerebral vasospasm. Neurol Res. 2009;31:568–81.
12. Sugawara T, Ayer R, Jadhav V, Zhang JH. A new grading system evaluating bleeding scale in filament perforation subarachnoid hemorrhage rat model. J Neurosci Methods. 2008;167:327–34.
13. Suzuki H, Kanamaru K, Tsunoda H, Inada H, Kuroki M, Sun H, et al. Heme oxygenase-1 gene induction as an intrinsic regulation against delayed cerebral vasospasm in rats. J Clin Invest. 1999;104:59–66.
14. Suzuki H, Hasegawa Y, Chen W, Kanamaru K, Zhang JH. Recombinant osteopontin in cerebral vasospasm after subarachnoid hemorrhage. Ann Neurol. 2010;68:650–60.
15. Suzuki H, Ayer R, Sugawara T, Chen W, Sozen T, Hasegawa Y, et al. Protective effects of recombinant osteopontin on early brain injury after subarachnoid hemorrhage in rats. Crit Care Med. 2010;38:612–8.
16. Chiquet-Ehrismann R, Matsuoka Y, Hofer U, Spring J, Bernasconi C, Chiquet M. Tenascin variants: differential binding to fibronectin and distinct distribution in cell cultures and tissues. Cell Regul. 1991;2:927–38.
17. Bennett SA, Tenniswood M, Chen JH, Davidson CM, Keyes MT, Fortin T, et al. Chronic cerebral hypoperfusion elicits neuronal apoptosis and behavioral impairment. Neuroreport. 1998;9:161–6.
18. Li Y, Lei Z, Xu ZC. Enhancement of inhibitory synaptic transmission in large aspiny neurons after transient cerebral ischemia. Neuroscience. 2009;159:670–81.
19. Yatsushige H, Ostrowski RP, Tsubokawa T, Colohan A, Zhang JH. Role of c-Jun N-terminal kinase in early brain injury after subarachnoid hemorrhage. J Neurosci Res. 2007;85:1436–48.
20. Macdonald RL, Kassell NF, Mayer S, Ruefenacht D, Schmiedek P, Weidauer S, et al. Clazosentan to overcome neurological ischemia and infarction occurring after subarachnoid hemorrhage (CONSCIOUS-1): randomized, double-blind, placebo-controlled phase 2 dose-finding trial. Stroke. 2008;39:3015–21.
21. Macdonald RL, Higashida RT, Keller E, Mayer SA, Molyneux A, Raabe A, et al. Clazosentan, an endothelin receptor antagonist, in patients with aneurysmal subarachnoid haemorrhage undergoing surgical clipping: a randomised, double-blind, placebo-controlled phase 3 trial (CONSCIOUS-2). Lancet Neurol. 2011;10:618–25.
22. Macdonald RL, Higashida RT, Keller E, Mayer SA, Molyneux A, Raabe A, et al. Randomized trial of clazosentan in patients with aneurysmal subarachnoid hemorrhage undergoing endovascular coiling. Stroke. 2012;43:1463–9.
23. Chiquet M, Sarasa-Renedo A, Tunc-Civelek V. Induction of tenascin-C by cyclic tensile strain versus growth factors: distinct contributions by Rho/ROCK and MAPK signaling pathways. Biochim Biophys Acta. 2004;1693:193–204.
24. Hindermann W, Berndt A, Borsi L, Luo X, Hyckel P, Katenkamp D, et al. Synthesis and protein distribution of the unspliced large tenascin-C isoform in oral squamous cell carcinoma. J Pathol. 1999;189:475–80.
25. Midwood KS, Orend G. The role of tenascin-C in tissue injury and tumorigenesis. J Cell Commun Signal. 2009;3:287–310.
26. Tredici G, Miloso M, Scuteri A, Foudah D. MAPKs as mediators of cell fate determination: an approach to neurodegenerative diseases. Curr Med Chem. 2008;15:538–48.

27. Lin CL, Dumont AS, Tsai YJ, Huang JH, Chang KP, Kwan AL, et al. 17β-estradiol activates adenosine A(2a) receptor after subarachnoid hemorrhage. J Surg Res. 2009;157:208–15.
28. Kusaka G, Ishikawa M, Nanda A, Granger DN, Zhang JH. Signaling pathways for early brain injury after subarachnoid hemorrhage. J Cereb Blood Flow Metab. 2004;24:916–25.
29. Ishigaki T, Imanaka-Yoshida K, Shimojo N, Matsushima S, Taki W, Yoshida T. Tenascin-C enhances crosstalk signaling of integrin αvβ3/PDGFR-β complex by SRC recruitment promoting PDGF-induced proliferation and migration in smooth muscle cells. J Cell Physiol. 2010;226:2617–24.
30. Wang HH, Hsieh HL, Yang CM. Calmodulin kinase II-dependent transactivation of PDGF receptors mediates astrocytic MMP-9 expression and cell motility induced by lipoteichoic acid. J Neuroinflammation. 2010;7:84.
31. Smits A, Kato M, Westermark B, Nister M, Heldin CH, Funa K. Neurotrophic activity of platelet-derived growth factor (PDGF): rat neuronal cells possess functional PDGF β-type receptors and respond to PDGF. Proc Natl Acad Sci U S A. 1991;88:8159–63.
32. Nishio T, Kawaguchi S, Iseda T, Kawasaki T, Hase T. Secretion of tenascin-C by cultured astrocytes: regulation of cell proliferation and process elongation. Brain Res. 2003;990:129–40.
33. Peng B, Dutreix C, Mehring G, Hayes MJ, Ben-Am M, Seiberling M, et al. Absolute bioavailability of imatinib (Glivec®) orally versus intravenous infusion. J Clin Pharmacol. 2004;44:158–62.
34. Breedveld P, Pluim D, Cipriani G, Wielinga P, van Tellingen O, Schinkel AH, et al. The effect of Bcrp1 (Abcg2) on the in vivo pharmacokinetics and brain penetration of imatinib mesylate (Gleevec): implications for the use of breast cancer resistance protein and P-glycoprotein inhibitors to enable the brain penetration of imatinib in patients. Cancer Res. 2005;65:2577–82.
35. El-Karef A, Yoshida T, Gabazza EC, Nishioka T, Inada H, Sakakura T, et al. Deficiency of tenascin-C attenuates liver fibrosis in immune-mediated chronic hepatitis in mice. J Pathol. 2007;211:86–94.